Frequency domain modeling and simulation of low voltage electric power networks with nonlinear loads

Summary of PHD thesis

PhD candidate

Eng. Valentin Ștefănescu

Scientific Advisor

Prof. Dr. Eng. Florin Constantinescu

Polytechnic University of Bucharest, Electrical Engineering Doctoral School

2021

DOCTORAL PAPER CONTENTS

Keywords: frequency domain analysis, current harmonics, nonlinear devices, interpolation algorithms, firing angle, thyristor.

3. NEW MODELS FOR FREQUENCY DOMAIN SIMULATION OF HOME APPLIANCES NETWORKS

3.1. INTRODCTION

Modern AC home appliances networks include nonlinear components as various types of illumination equipment, microwave ovens, vacuum cleaners and others. All these devices have a nonlinear behavior as well as various types of inverters and converters associated to clean energy sources. Moreover, the home appliances network is usually a part of an AC power system containing distributed parameters components like transmission lines, compensation capacitors with high capacity values and transformers with high inductance values.

Starting from a property of phases of the current harmonics described in [13], and knowing that in a power system the voltage fundamental component of a consumer cannot be outside the interval [0.9 V_n 1.1 V_n], where V_n is its nominal value, linear frequency domain models of one diode and two diodes rectifiers powering compact fluorescent lamps (CFL) have been proposed in [19]. These models have been obtained starting from simulations using the CFL model in [21]. For example, the third current harmonic is described in this model as:

$$I_3 = polar\big(1.024e - 3 * mag(V_1), 94 + 3 * phase(V_1)\big) \quad (3.2)$$

This description is made in the language of ADS, where V_1 is the voltage fundamental component. Similar models, obtained from measured results, are described in [22]. The measurement results have only two digits being read from the power analyser screen.

New frequency domain (FD) models of home appliance devices are presented in Section 3.2.

3.2. NEW FD MODELS OF HOME APPLIANCES

The following models are established by measuring the harmonic components of the current (rms value and phase) with a power analyzer. These measurements have been performed in the ranges of [190 V, 250 V] or [200 V, 240 V], The diagrams are drawn using a linear interpolation, according to the relation (3.2).

A. Compact fluorescent lamps (CFL) and light emission diodes (LED)

TABLE 3.1. **Current Harmonics Rms And Phases For CFL 10 W [28]**

RMS [A]	PHASE [deg]
$rms(I_1) = -5E\text{-}18\ V_1 + 6E\text{-}2$	$ph(I_1) = 0$
$rms(I_3) = 3E\text{-}5\ V_1 + 4E\text{-}2$	$ph(I_3) = -2.8E\text{-}2\ \Phi_1 + 184$
$rms(I_5) = 4E\text{-}5\ V_1 + 2.2E\text{-}2$	$ph(I_5) = -0.11\ \Phi_1 + 35$
$rms(I_7) = 1E\text{-}6\ V_1 + 2.4E\text{-}2$	$ph(I_7) = -0.17\ \Phi_1 - 102$
$rms(I_9) = 7E\text{-}6\ V_1 + 2.1E\text{-}2$	$ph(I_9) = -0.14\ \Phi_1 + 90$
$rms(I_{11}) = 3E\text{-}5\ V_1 + 1E\text{-}2$	$ph(I_{11}) = -0.21\ \Phi_1 - 55$
$rms(I_{13}) = 2E\text{-}7\ V_1 + 1.3E\text{-}2$	$ph(I_{13}) = -0.38\ \Phi_1 + 193$
$rms(I_{15}) = -2E\text{-}5\ V_1 + 1.6E\text{-}2$	$ph(I_{15}) = -0.27\ \Phi_1 + 20$
$rms(I_{17}) = 6E\text{-}6\ V_1 + 9.3E\text{-}3$	$ph(I_{17}) = -0.3\ \Phi_1 + 228$

Please take into account that $\Phi_1 = phase(V_1)$. The term $k*\ phase(V_1)$ must be added for all models in the phase formula of $ph(I_k)$.

All measurement results in Section 3.2. have been obtained using the acquisition program Power Analyzer Transfer 3.07 employing four digits. This leads to better precision characteristics than those in [22].

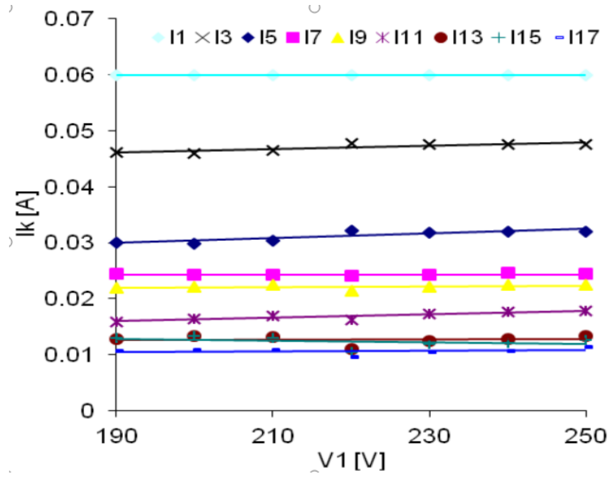

Fig. 3.1. Current harmonics rms vs. V_1 for CFL 10W [28]

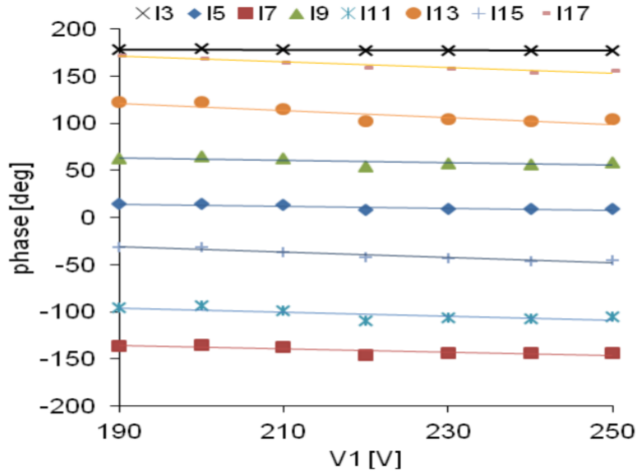

Fig. 3.2. Current harmonics phases vs. V_1 for CFL 10W [28]

Table 3.2. **Current Harmonics RMS And Phases For LED 5W** [28]

RMS [A]	PHASE [deg]
$rms(I_1) = 0.2$	$ph(I_1) = 0$
$rms(I_3) = 2E\text{-}5\ V_1 + 1.3E\text{-}2$	$ph(I_3) = -0.06\ \Phi_1 + 186$
$rms(I_5) = 4E\text{-}5\ V_1 + 4.6E\text{-}3$	$ph(I_5) = -0.17\ \Phi_1 + 33$
$rms(I_7) = 3E\text{-}5\ V_1 + 2.7\ E\text{-}3$	$ph(I_7) = -0.39\ \Phi_1 - 83$
$rms(I_9) = 1E\text{-}5\ V_1 + 5.3E\text{-}3$	$ph(I_9) = -0.49\ \Phi_1 + 136$
$rms(I_{11}) = 2E\text{-}5\ V_1 + 3.2E\text{-}3$	$ph(I_{11}) = -0.48\ \Phi_1 - 33$
$rms(I_{13}) = 3E\text{-}5\ V_1 - 8.2E\text{-}4$	$ph(I_{13}) = -0.64\ \Phi_1 + 197$
$rms(I_{15}) = 2E\text{-}5\ V_1 - 2.8E\text{-}4$	$ph(I_{15}) = -0.95\ \Phi_1 + 106$
$rms(I_{17}) = 2E\text{-}5\ V_1 - 1.1E\text{-}3$	$ph(I_{17}) = -0.98\ \Phi_1 + 315$

Table 3.3. **Current Harmonics RMS And Phases For LED 17W** [28]

RMS [A]	PHASE [deg]
$rms(I_1) = -3.9E\text{-}4\ V_1 + 1.6E\text{-}1$	$ph(I_1) = 0$
$rms(I_3) = -2.3E\text{-}4\ V_1 + 1.2E\text{-}1$	$ph(I_3) = -3.9E\text{-}2\ \Phi_1 + 185$
$rms(I_5) = -5E\text{-}5\ V_1 + 6\ E\text{-}2$	$ph(I_5) = -0.17\ \Phi_1 + 38$
$rms(I_7) = -2E\text{-}5\ V_1 + 4E\text{-}2$	$ph(I_7) = -0.44\ \Phi_1 - 67$
$rms(I_9) = -8E\text{-}5\ V_1 + 4.6E\text{-}2$	$ph(I_9) = -0.54\ \Phi_1 + 157$
$rms(I_{11}) = -3E\text{-}5\ V_1 + 3.2E\text{-}2$	$ph(I_{11}) = -0.55\ \Phi_1 - 5$
$rms(I_{13}) = 4E\text{-}5\ V_1 + 1.1E\text{-}2$	$ph(I_{13}) = -0.77\ \Phi_1 + 241$
$rms(I_{15}) = 7E\text{-}6\ V_1 + 1.4E\text{-}2$	$ph(I_{15}) = -1.11\ \Phi_1 + 157$
$rms(I_{17}) = 2E\text{-}5\ V_1 + 6.5E\text{-}3$	$ph(I_{17}) = -1.12\ \Phi_1 + 362$

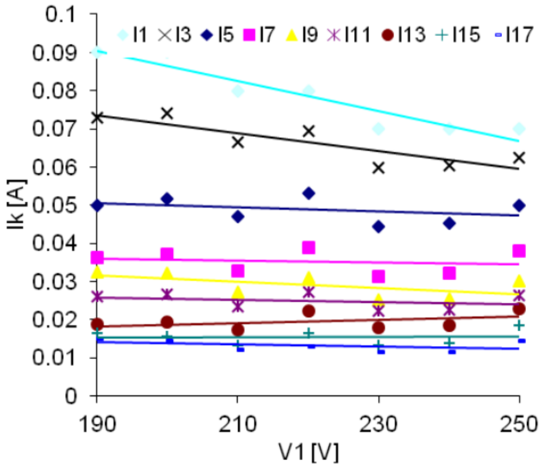

Fig. 3.3. Current harmonics rms vs. V_1 for LED 17W [28]

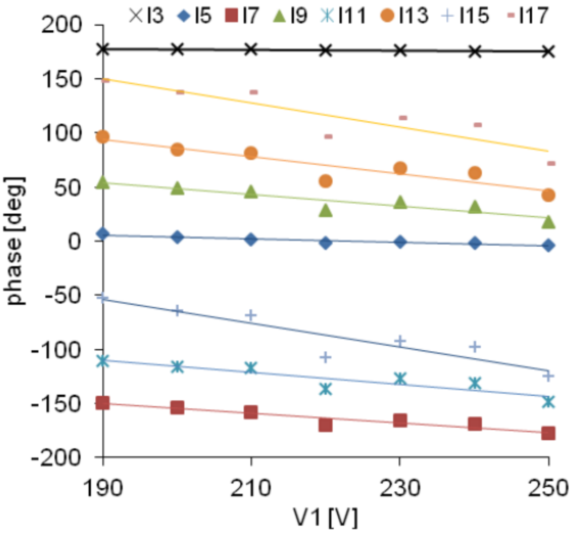

Fig. 3.4. Current harmonics phases vs. V_1 for LED 17W [28]

Some models have also been built for the following non-linear consumers: air conditioning (heating), air conditioning (cooling), vacuum cleaner (maximum power, loaded), vacuum cleaner (average power, loaded), vacuum cleaner (minimum power, loaded), vacuum cleaner (minimum power, unloaded), vacuum cleaner (average power, unloaded), vacuum cleaner (minimum power, unloaded) and a refrigerator (closed door).

4. FREQUENCY DOMAIN MODELS FOR NONLINEAR LOADS WITH FIRING ANGLE CONTROL DEVICES - MEASUREMENTS

4.1. INTRODUCTION

Starting from the rule stating that the fundamental voltage component of any consumer must belong to [0.9 V_n, 1.1 V_n], where V_n is the nominal value of this voltage, it seems that any harmonic current source can be described by a small signal model including linear dependences on the fundamental voltage component parameters only as [19]:

$$\begin{aligned} I_1 &= polar\left(1.276e-3*mag(V_1), 31+1*phase(V_1)\right) \\ I_3 &= polar\left(1.024e-3*mag(V_1), 94+3*phase(V_1)\right) \\ I_5 &= polar\left(6.453e-4*mag(V_1), 164+5*phase(V_1)\right) \end{aligned} \tag{4.1}$$

where each harmonic current is described by its amplitude (*mag*) - phase (*phase*) pair. The parameters of these models have been computed by simulations using some reduced order equivalent circuits of the compact fluorescent lamps [19].

This chapter deals with the frequency domain models of nonlinear loads with firing angle control devices. The conduction state of the devices as thyristors, IGBTs (insulated gate bipolar transistors), TRIACs (triodes for alternating current), DIACs (diodes for alternating current) is controlled by a command signal [31]. Some measurements on one phase and three phase thyristor rectifiers, which will lead to their frequency domain models, are reported in this chapter.

Section 4.2 presents a method based on a genetic algorithm which develops a more appropriate harmonic decomposition for periodic function defined by a set of samples, than the usual algorithms implemented on network analyzers. The measurements results for a one phase rectifier are given in Section 4.3, while the data obtained for a three-phase rectifier are reported in Section 4.4.

4.2. HARMONICS PARAMETERS IDENTIFICATION

We improved the procedure implemented into FLUKE 435 analyzer for the harmonics modules and phases computation using the algorithm described in [32].

The approximation of a current waveform in a three phase rectifier using both methods shows that the genetic algorithm leads to a better waveform reconstruction than the procedure of the FLUKE 435 network analyzer (Fig. 4.1).

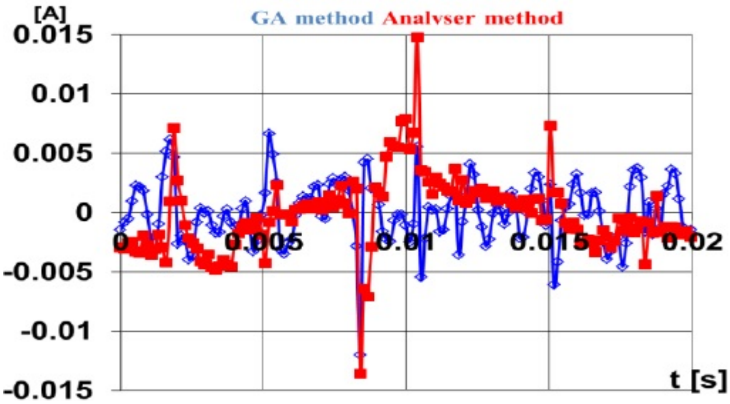

Fig. 4.1. Absolute error for all samplEs for a current waveform in a three phase resonator [33]

4.3. RESULTS FOR A ONE PHASE RECTIFIER WITH ONE THYRISTOR

The schematic of this rectifier is given in Fig. 4.2 a.

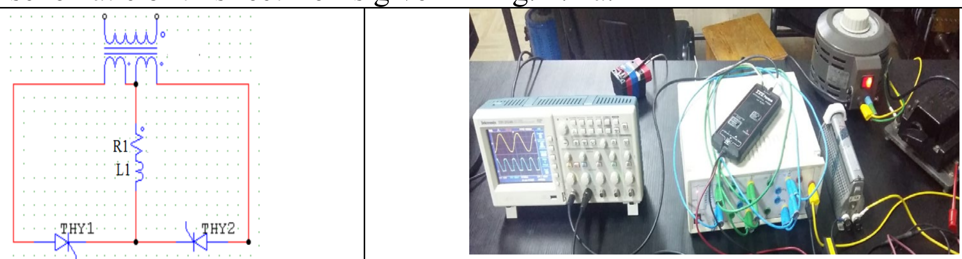

a

b

Fig. 4.2. One phase rectifier a) Schematic, b) Measurement setup [33]

The measurement setup is shown in Fig. 4.2.b. The current harmonics amplitudes and phases dependences on the fundamental component of the voltage are measured for various values of the firing angle (Figures 4.3-4.14).

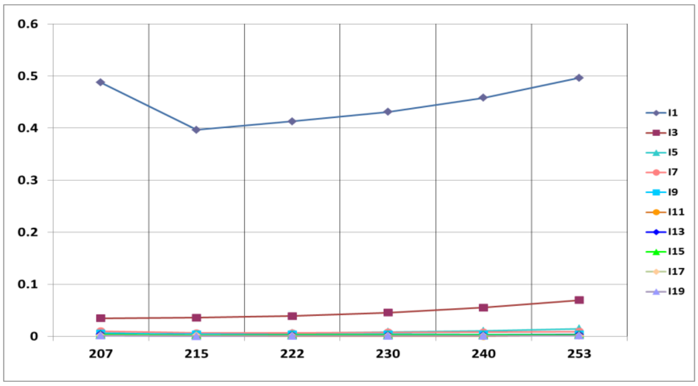

Fig. 4.3. RMS values for I_1 –I_{19} [A] for α=21 grd [33]

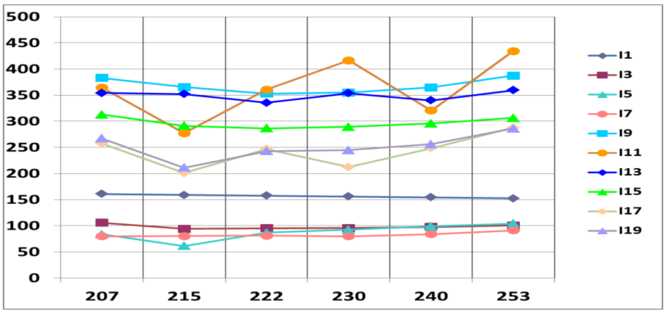

Fig. 4.4. PHASE values for I_1 –I_{19} for α=21 grd [33]

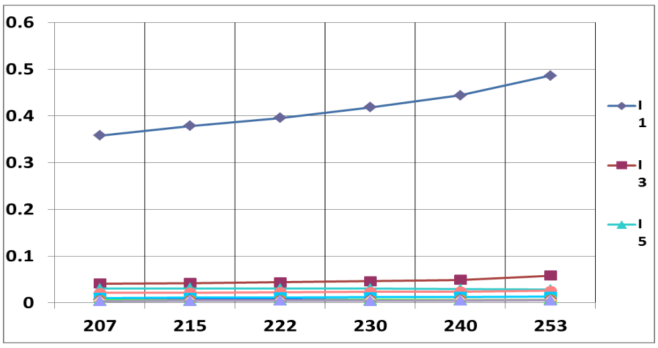

Fig. 4.5. RMS value for I_1 –I_{19} [A] for α=50 grd [33]

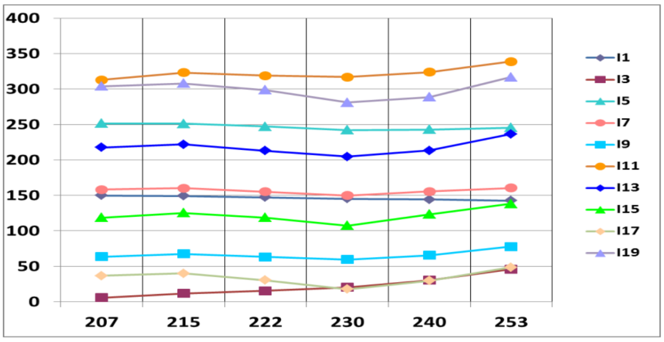

Fig. 4.6 PHASE value for I_1 –I_{19} for α=50 grd [33]

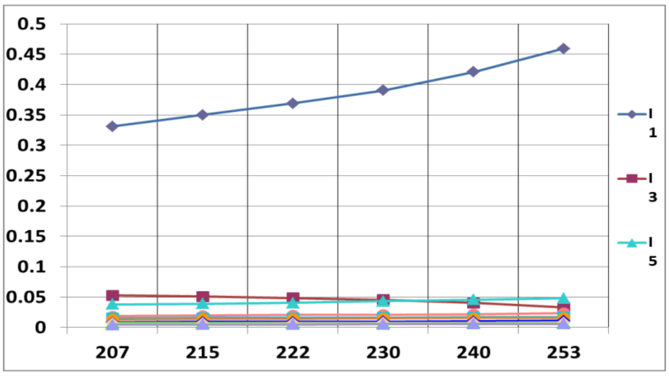

Fig. 4.7. RMS value for I_1 –I_{19} [A] for α=70 grd [33]

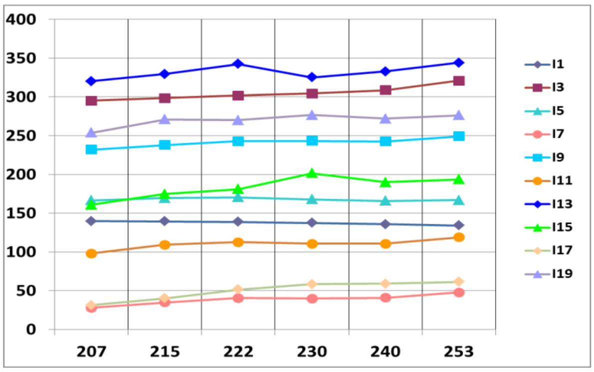

Fig. 4.8. PHASE value for I_1 –I_{19} for α=70 grd [33]

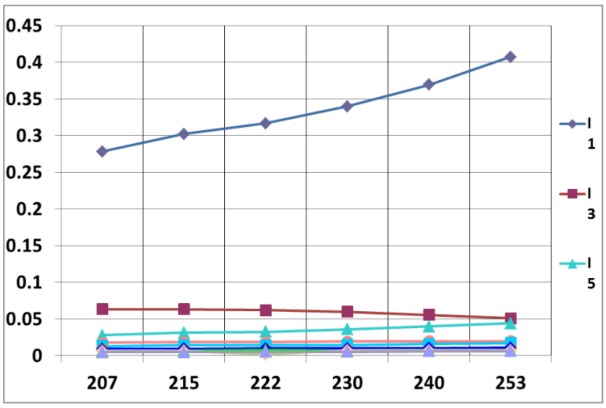

Fig. 4.9. RMS value for I_1 –I_{19} [A] for α=90 grd [33]

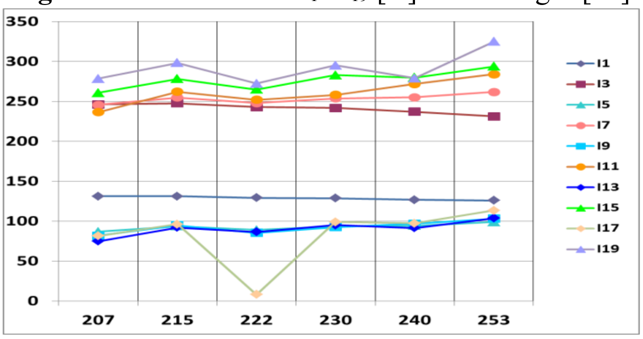

Fig. 4.10. PHASE value for I_1 –I_{19} for α=90 grd [33]

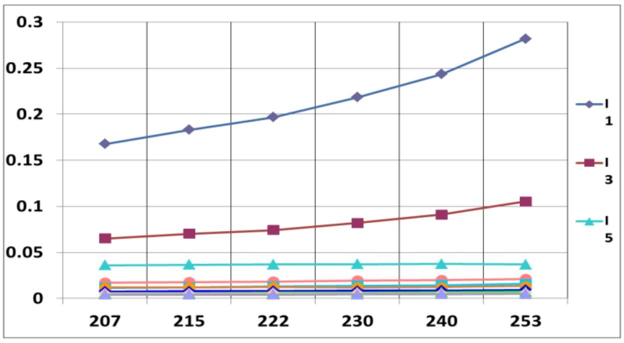

Fig. 4.11. RMS value for I_1 –I_{19} [A] for α=126 grd [33]

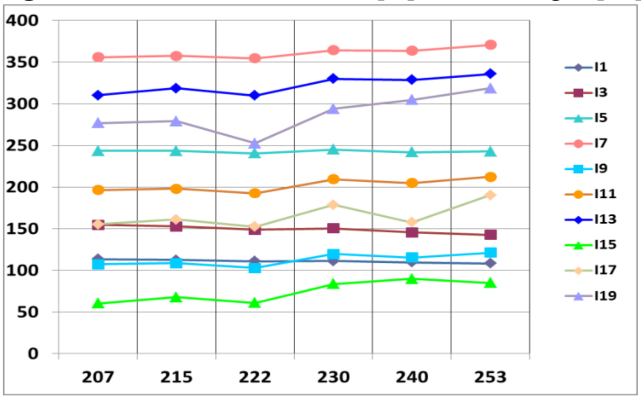

Fig. 4.12. PHASE value for I_1 –I_{19} for α=126 grd [33]

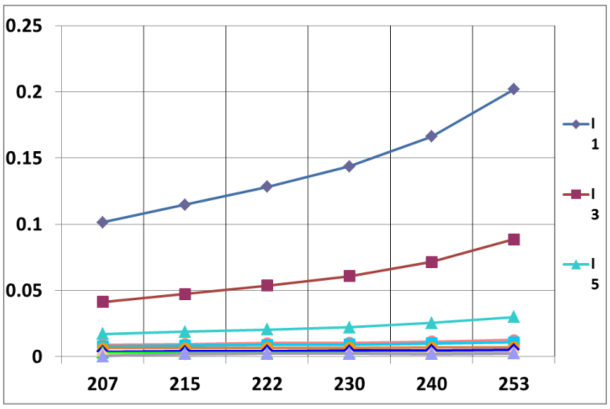

Fig. 4.13. RMS value for I_1 –I_{19} [A] for α=150 grd [33]

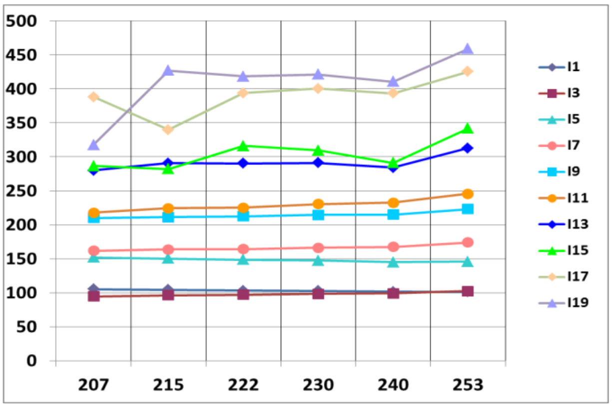

Fig. 4.14. PHASE value for I_1 –I_{19} for α=150 grd [33]

Similar results have been obtained for a three-phase rectifier.

5. FREQUENCY DOMAIN MODELS FOR NONLINEAR LOADS WITH FIRING ANGLE CONTROL DEVICES - MODELING

5.1. INTRODUCTION

In the previous chapter the measurements of a one phase rectifier with one thyristor and of a three-phase rectifier with three thyristors [33] have been reported by the authors. Our target, to build frequency domain models for this kind of circuits, is accomplished in this chapter for a one phase rectifier with one thyristor.

The measured results are described in [33] and consist in the dependence of the RMS value and phase value of the odd harmonics (from the first one to the 19-st) on V_1 and phase (V_1) and on the firing angle control of the thyristor. In this paper we will consider only the first six odd current harmonics and their RMS and phase dependence measured for the values of V_1 and of the firing angle α given in the tables below.

Table 5.1. **V_1 values** [34]

U_1 [V]	U_2 [V]	U_3 [V]	U_4 [V]	U_5 [V]	U_6 [V]
207	215	222	230	240	253

Table 5.2. **α values** [34]

α_1 [°]	α_2 [°]	α_3[°]	α_4 [°]	α_5 [°]	α_6 [°]
21	50	70	90	126	150

An useful model must compute the dependencies of the RMS and phase values of each current harmonic component on V_1 and *phase (V_1)* for a new firing angle knowing the measured dependencies for a set of firing angles.

Our proposed model will be a polynomial in one variable (V_1 or *phase (V_1)*) because this kind of expression can be easily implemented in the Advanced Design System (ADS) software which uses the most powerful variant of the HB method. In order to verify the validity of our approach we ignore the measured values for α_3=70° and try to compute them using two interpolation polynomials. The first interpolation polynomial is given by the poly45 function of MATLAB; this polynomial is computed using four values for α and five values for V_1. The second interpolation polynomial, presented in chapter 5.2, employs five values for α and six values for V_1. Chapter 5.3 contains the results obtained with these interpolation polynomials, namely the dependencies of the first six odd current harmonics RMS values and phases on V_1 for α_3=70°. These dependencies are compared with those computed employing a genetic algorithm, from the measured current samples so that the best current waveform is rebuilt [32]. Chapter 5.4 contains the conclusions, showing which interpolation polynomial is the most suited for our purpose.

5.2. INTERPOLATION ALGORITHM

Starting from the measured current samples $i_j = i(t_j), j = \overline{1,S}$, the RMS values I_{2k-1} and initial phases φ_{2k-1} for the fundamental component and the odd harmonics till the 11-th order $(k = \overline{1,6})$ are computed so that the sum of the above components be the best approximation of the measured current waveform:

$$i(t) = \sum_{k=1}^{6} \sqrt{2}\, I_{2k-1} \sin\big((2k-1)\varphi t + \varphi_{2k-1}\big) \tag{5.1}$$

To this end the following error function is defined:

$$ERR(I_1, \varphi_1, I_3, \varphi_3, \cdots, I_{11}, \varphi_{11}) = \sum_{i=1}^{S} \big[i_j - i(t_j)\big]^2 \tag{5.2}$$

Introducing (5.1) in (5.2) it follows:

$$ERR(I_1, \varphi_1, I_3, \varphi_3, \cdots, I_{11}\varphi_{11}) = \sum_{i=1}^{S}\left[i_j - \sum_{k=1}^{6}\sqrt{2}\, I_{2k-1}\sin\left((2k-1)\varphi t_j + \varphi_{2k-1}\right)\right]^2 \quad (5.3)$$

This error function has twelve variables, so that a solution vector x with twelve components is defined in order to minimize the value of above function with MATLAB. The correspondence between the solution vector and the components of x is:

$$A_{2k-1} \to x_{2k-1}, \varphi_{2k-1} \to x_{2k}, k = \overline{1,6} \quad (5.4)$$

Employing (5.4) in (5.3) we obtain:

$$ERR(x_1, x_2, \cdots, x_{11}, x_{12}) = \sum_{j=1}^{S}\left[i_j - \sum_{k=1}^{6}\sqrt{2}\, x_{2k-1}\sin\left((2k-1)\varphi t_j + x_{2k}\right)\right]^2 \quad (5.5)$$

The error function in (5.5) is generated with MAPLE and is converted in the MATLAB code. This error function value is minimized with the MATLAB function `ga` from Global Optimization Toolbox. This minimization procedure employs genetic algorithms leading to the RMS values and phases of the odd harmonic components of orders 1-11. To this end the following options are used for the `ga` function: 'HybridFcn', @fminunc, 'Generations', 1200, 'TolFun', 1e-15.

By this way the algorithm computes the RMS and initial phase values of the 6 odd current harmonic components for a set of *MxN* points defined by the fundamental voltage component values $U_m, m = \overline{1,M}$ and the firing angle values $\alpha_n, n = \overline{1,N}$.

In order to compute the same RMS and initial phase values of the 6 odd harmonic components in a new point, the polynomial interpolation described below is employed. Namely, in order to compute the RMS value I_k and the initial phase φ_k of the k-th current harmonic two interpolation polynomials of the order $(M-1)\times(N-1)$ are built. These are the following two variable polynomials in U and α:

$$\begin{aligned} P_{I_k}(U,\alpha) &= \sum_{i=1}^{M}\left(U^{i-1}\sum_{j=1}^{N}A_{j+(i-1)\cdot N}\alpha^{j-1}\right) = \\ &= A_1 + A_2\alpha + \cdots A_N\alpha^{N-1} + A_{N+1}U + \cdots + A_{2N}U\alpha^{N-1} + \\ &\dots + A_{1+(M-1)\cdot N}U^{M-1} + \cdots + A_{M\cdot N}U^{M-1}\alpha^{N-1} \end{aligned} \quad (5.6)$$

$$\begin{aligned} P_{\varphi_k}(U,\alpha) &= \sum_{i=1}^{M}\left(U^{i-1}\sum_{j=1}^{N}B_{j+(i-1)\cdot N}\alpha^{j-1}\right) = \\ &= B_1 + B_2\alpha + \cdots B_N\alpha^{N-1} + B_{N+1}U + \cdots + B_{2N}U\alpha^{N-1} + \\ &\dots + B_{1+(M-1)\cdot N}U^{M-1} + \cdots + B_{M\cdot N}U^{M-1}\alpha^{N-1} \end{aligned} \quad (5.7)$$

These polynomials are built so that their evaluation gives the RMS value of I_k and the initial phase of I_k corresponding to the fundamental voltage component U_m and to the firing angle α_n:

$$P_{I_k}(U_m,\alpha_n) = \sum_{i=1}^{M}\left(U_m^{i-1}\sum_{j=1}^{N}A_{j+(i-1)\cdot N}\alpha_n^{j-1}\right) = I_k(U_m,\alpha_n) \quad (5.8)$$

$$P_{\varphi_k}(U_m,\alpha_n) = \textstyle\sum_{i=1}^{M}\left(U_m^{i-1}\sum_{j=1}^{N}B_{j+(i-1)\cdot N}\alpha_n^{j-1}\right) = \varphi_k(U_m,\alpha_n). \quad (5.9)$$

The computation of the coefficients $A_{j+(i-1)\cdot N}$, respective $B_{j+(i-1)\cdot N}$, $i=\overline{1,M}$, $j=\overline{1,N}$, is done by solving the following equation systems

:

$$\begin{aligned} &A_1 + A_2\alpha_n + \cdots + A_{j+(i-1)\cdot N}U_m^{i-1}\alpha_n^{j-1} + \cdots + A_{M\cdot N}U_m^{M-1}\alpha_n^{N-1} == I_k(U_m,\alpha_n), \\ &m = \overline{1,M}, n = \overline{1,N}, \left(i = \overline{1,M}, j = \overline{1,N}\right) \end{aligned} \quad (5.11)$$

$$B_1 + B_2\alpha_n + \cdots + B_{j+(i-1)\cdot N}U_m^{i-1}\alpha_n^{j-1} + \cdots + B_{M\cdot N}U_m^{M-1}\alpha_n^{N-1} == \varphi_k(U_m, \alpha_n),$$
$$m = \overline{1,M}, n = \overline{1,N}, \left(i = \overline{1,M}, j = \overline{1,N}\right) \tag{5.12}$$

Knowing the values of the coefficients $A_{j+(i-1)\cdot N}$ and $B_{j+(i-1)\cdot N}$ for $i = \overline{1,M}$ și $j = \overline{1,N}$, the algorithm computes the RMS value and the initial phase of the k-th current harmonic in a point corresponding to the fundamental voltage RMS value *U'*, $U_1 \leq U' \leq U_M$, and to the firing angle *α'*, $\alpha_1 \leq \alpha' \leq \alpha_N$, as:

$$I_k(U',\alpha') = P_{I_k}(U',\alpha') = \sum_{i=1}^{M}\sum_{j=1}^{N} A_{j+(i-1)\cdot N}\alpha'^{\,j-1}U'^{\,i-1} \tag{5.13}$$

$$\varphi_k(U',\alpha') = P_{\varphi_k}(U',\alpha') = \sum_{i=1}^{M}\sum_{j=1}^{N} B_{j+(i-1)\cdot N}\alpha'^{\,j-1}U'^{\,i-1} \tag{5.14}$$

In order to compare the results, the magnitudes in (5.13) and (5.14) are computed with the function fit from the Curve Fitting Toolbox of MATLAB. The parameter fitType is „poly45" and in this case the polynomial has the order 4x5. its variables being α_n U_m. Obviously the FD models are the curves $I_k(U_m, \alpha_n)_{\alpha n=ct}$ and $\varphi_k(U_m, \alpha_n)_{\alpha n=ct}$ obtained from (5.8) and (5.9) or from (5.13) and (5.14). These are polynomials in Um and may be considered as a generalization of the linear models in (5.1). This kind of models can be easily implemented in ADS.

5.3. RESULTS

In the following the performances of the models obtained with the poly45 function (MATLAB) and with the polynomial interpolation described in Section 5.2 are illustrated. Firstly the RMS value of the fundamental current component dependence on *U* and α is shown by the red points in Fig. 5.1.

This dependence is compared with that given by the genetic algorithm in [32] starting from the measured time samples (green points). Without the measured data for α=70° the measured points correspond to 6 values for *U* and 5 values for α, so the poly4 function chooses the most appropriate 20 points to build the interpolation polynomials (blue points).

This dependence is compared with that given by the genetic algorithm in [32] starting with the measured time samples (green dots). Without the measured data for α = 70˚, the points obtained from the measurements correspond to a number of six values for U and five values for α, so that the poly45 function chooses the most suitable twenty points for the construction of interpolation polynomials (blue dots).

A measure of the error of this interpolation method is given by the distances between the green and the red point in each pair.

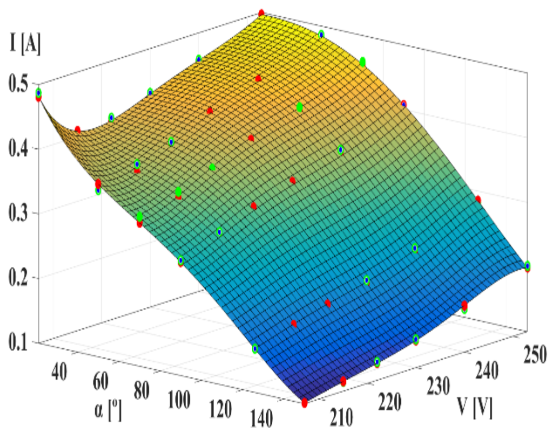

Fig. 5.1. First harmonic RMS value vs. U and α (poly45) [34]

A similar measure of the interpolation error is given in Fig. 5.2 for the initial phase of the fundamental component of the current computed with poly45 (MATLAB)

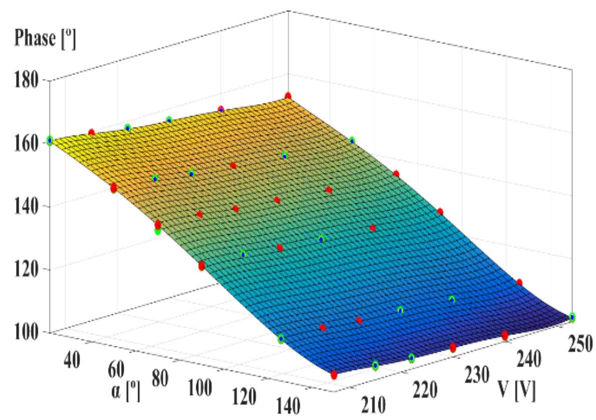

Fig. 5.2. First harmonic initial phase value vs. U and α (poly45) [34]

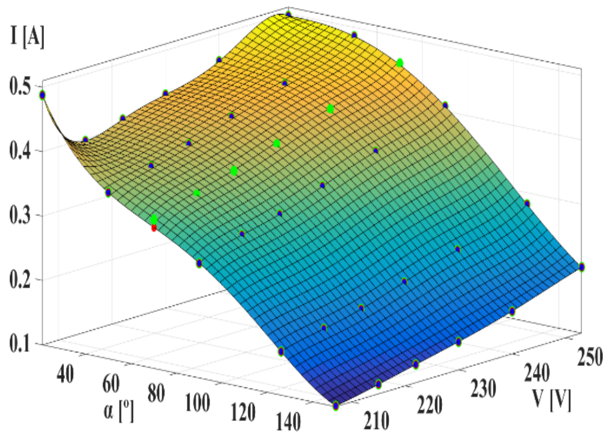

Fig. 5.3. First harmonic RMS value vs. U and α (proposed interpolation) [34]

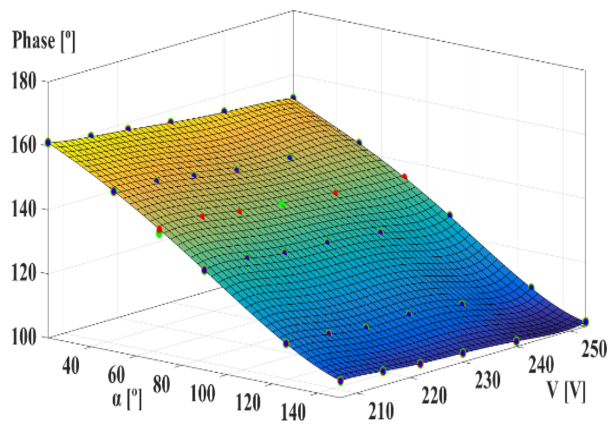

Fig. 5.4. First harmonic initial phase value vs. U and α (proposed interpolation) [34]

The errors of the proposed interpolation method can be estimated analyzing Fig. 5.1- Fig. 5.4. A simple examination of the distances between the green and the red point in each pair shows that the proposed interpolation gives better results than the poly45 function (MATLAB).

In the following the RMS values and initial phase values dependences on U for all odd current harmonics obtained by both interpolation algorithms for α= 70^0 are compared with the same dependences given by the genetic algorithm in [32], which are based on the measured time samples and are considered the minimum error data.

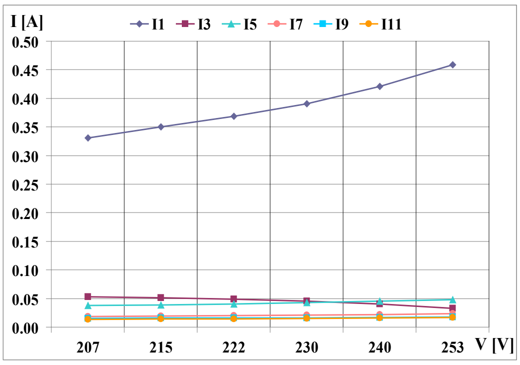

Fig. 5.5. RMS values vs. U for $\alpha = 70^{\circ}$ obtained with the genetic algorithm [34]

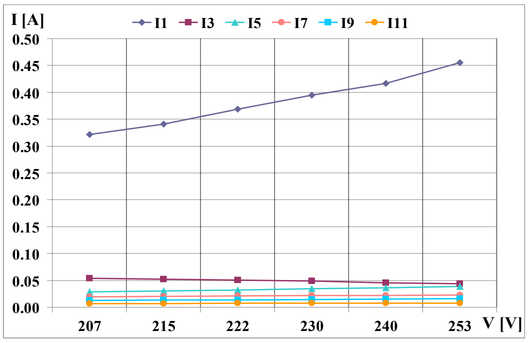

Fig. 5.6. RMS values vs.U for $\alpha = 70^{\circ}$ obtained with poly45 (MATLAB) [34]

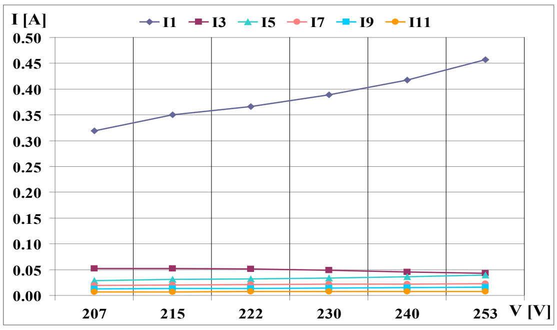

Fig. 5.7. RMS values vs. U for $\alpha = 70^{\circ}$ obtained with the proposed interpolation [34]

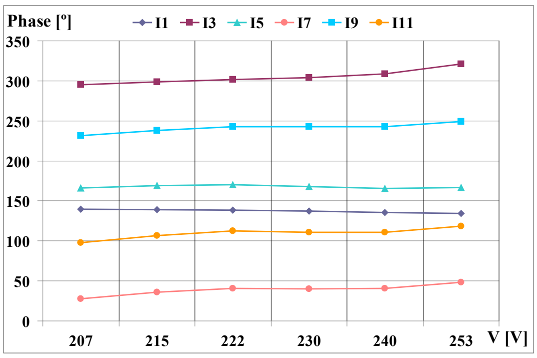

Fig. 5.8. Initial phases vs. U fir $\alpha = 70^{\circ}$ obtained with the genetic algorithm [34]

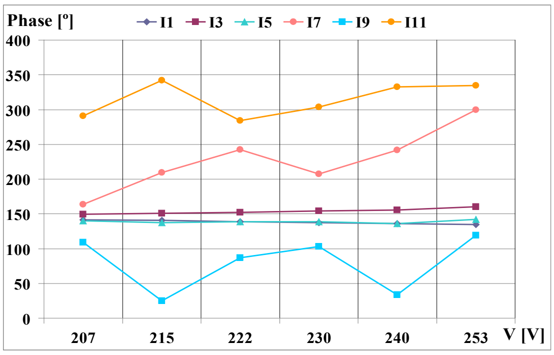

Fig. 5.9. Initial phases vs. U for $\alpha = 70^{\circ}$ obtained with poly45 (MATLAB) [34]

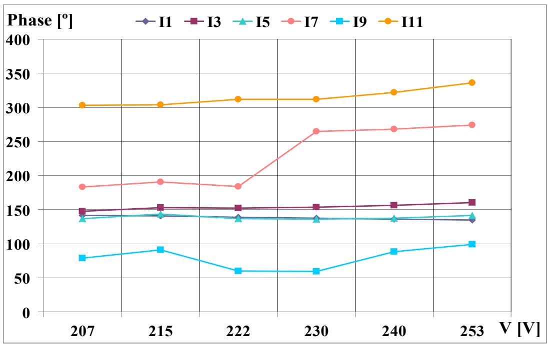

Fig. 5.10. Initial phases vs. U for $\alpha = 70^{\circ}$ obtained with the proposed interpolation [34]

A simple examination of the figures 5.5-5.7 shows that the results obtained with poly 45 function (MATLAB) and with the proposed interpolation algorithms are very close to those given by the genetic algorithm in [32] which is based on the measured time samples. From the figures 5.8-5.10 it is obvious that, unlike the RMS values, the initial phases obtained with poly 45 function (MATLAB) and with the proposed interpolation exhibit significant errors with respect to those given by the genetic algorithm in [32].

Another way of error estimation for various methods we have used is the waveform reconstruction. Fig. 5.11 presents the following current waveforms: measured (red line), reconstructed using the algorithm in [32] (blue line), reconstructed using poly45 interpolation (pink line), and reconstructed using the proposed polynomial interpolation (green line).

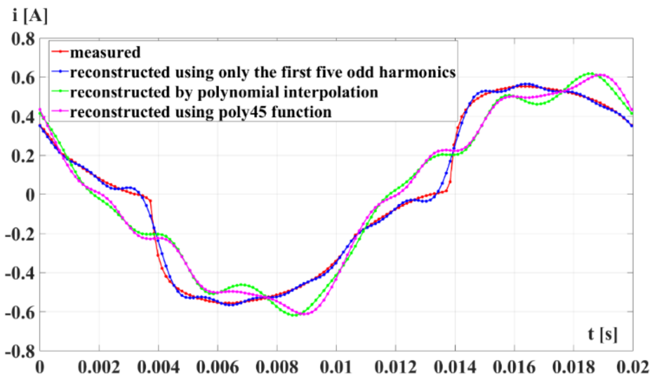

Fig. 5.11. Measured and reconstructed current waveforms for $\alpha = 70^{\circ}$ and $U = 230$V [34]

It is obvious that the use of the genetic algorithm in [32] leads to the closest waveform to the measured one.

In order to have a measure regarding this type of errors, Fig. 5.12 shows the spectrum of the RMS values for α= 70° and U=130V obtained employing both the poly 45 interpolation algorithm (red line) and the proposed interpolation algorithm (green line) in comparison with the spectrum corresponding to the RMS values calculated with the algorithm in [32] (blue line).

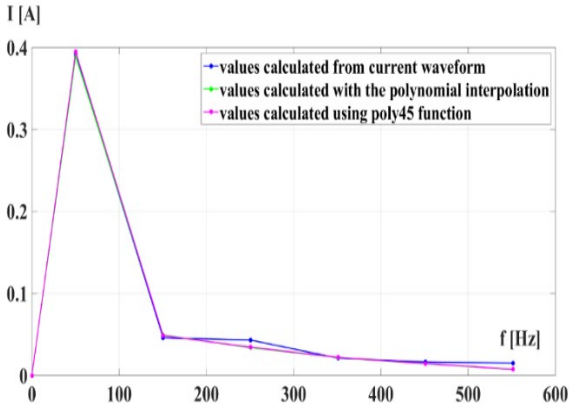

Fig. 5.12. RMS current harmonics spectrum [34]

At a first glance all these results are very close one another.

The phase spectrum computed for α= 70° and U=130V using the same algorithms is given in Fig. 5.13. In this case some important errors can be observed.

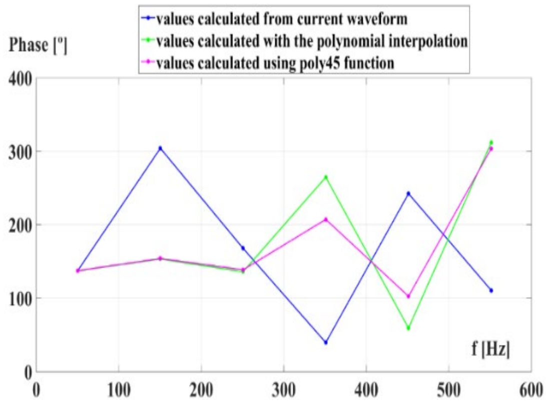

Fig. 5.13. Initial phase current harmonics spectrum [34]

7. CONCLUSIONS AND ORIGINAL CONTRIBUTIONS

7.1. OVERALL CONCLUSIONS

This thesis starts with a three-part introduction:

- *Non-sinusoidal steady state in power networks,* reviewing the main features of modern power networks in non-sinusoidal periodic steady state.

- *Analysis methods of power networks with non-linear loads,* describing the known analysis methods of nonlinear circuits using both classic methods (described by links between functions of time) and frequency domain models (consisting in dependencies of harmonic components of currents and voltages in relation to various parameters of the simulated circuit).

- *Frequency domain models and harmonic balance analysis of networks with nonlinear home appliances,* presenting the recent outcomes on frequency domain models for diode rectifiers and efficiency of harmonic balance analysis using these models. It is emphasized that the harmonic balance method implemented in ADS software using frequency domain models is more efficient than the ADS harmonic balance using time domain models.

Chapter 2 *Frequency domain models for nonlinear home appliance devices* presents the frequency domain models for several nonlinear home appliance devices (compact fluorescent lamps, an air conditioning system, a vacuum cleaner, a refrigerator and a microwave oven). These models are based on certain measurements made with a network analyzer displaying most significant two-digit RMS values and phases of harmonic components of the measured currents. The frequency domain models resulting from these measurements refer to the 1st, 3rd, 5th, 7th and 9th current harmonics parameters. These models have been implemented in ADS software and they have been used for the analysis of a three flats' network including these appliances in three variants: under symmetrical operation conditions, under slightly unbalanced conditions and under strongly unbalanced conditions. The elaborated models are characterized by the current harmonics' amplitudes and phases which are linearly depending on amplitude of the voltage fundamental component. These models are valid for the range [0,9 V_n, 1,1 V_n] where V_n is the RMS standard voltage value.

Chapter 3 presents new frequency domain models for several home appliance devices operating under various conditions. These models use linear dependencies of the RMS values and phases of the current harmonics in relation with the parameters of the voltage fundamental component. These dependencies have been measured within the voltage ranges [190 V, 250 V] or [200 V, 240 V]. These models have been elaborated faster than those presented in Chapter 2, as measurements were carried out using a network analyzer that provide the measured data in an Excel compatible format. The results of these measurements were delivered using four significant digits, which are more accurate than those used in the chapter 2 of this thesis. All models elaborated for the variation ranges of the voltage fundamental component mentioned above are represented using linear relationships, which are very easy to implement in ADS software.

In chapter 4, *Frequency domain models for nonlinear loads with firing angle control devices - measurements* new models are built for some nonlinear devices with thyristors. If the models from previous chapters contained only dependencies of the RMS values and phases of the current harmonics in relation with the voltage fundamental component, these new models also include the dependencies of these parameters on the firing angle. In paragraph 4.3 we present the results of the measurements of the dependencies on the voltage fundamental component for RMS values and phases of the current harmonics for six values of the firing angle of the two thyristors in a one-phase rectifier. In paragraph 4.4 we present the results of the measurements of the dependencies on the voltage fundamental component for RMS values and phases of the current harmonics for five values of the firing angle of the six thyristors. These measurements are made for several values of the voltage fundamental component within the range [0,9 V_n, 1,1 V_n], where V_n is its standard value. Analyzing these dependencies we notice that at least for certain values of the firing angle the linear models used in chapter 3 are unable to characterize the behavior of the rectifiers with thyristors.

In chapter 5, *Frequency domain models for nonlinear loads with firing angle control devices - modeling* we present the frequency domain model of a single-phase rectifier with two thyristors consisting in the dependencies of the RMS values and phases of the current harmonics with respect to the RMS value of the voltage fundamental component and the firing angle of the thyristors. These models start from the results of the measurements presented in chapter 4 which were conducted for six RMS values of the voltage fundamental component at the rectifier's terminals and for six firing angles. In order to prove the validity of the procedures for determining this model's parameters, we ignored the measured values for the firing angle α_3=70º. Later, the model parameters for α_3=70º were obtained by interpolating the results calculated for α_1=21º, α_2=50º, α_4=90º, α_5=126º and α_6=150º. The values obtained from this interpolation are virtually overlapping the measured values for α=70º. By this way we demonstrate the validity of the building method of this model. We used three calculation procedures for modules and phases of the current harmonics. The first procedure uses a genetic algorithm [32], the second procedure uses the *poly45* function in MATLAB and the third procedure uses an algorithm which is similar to *poly45* that leads to a two-variable polynomial whose coefficients are determined starting from measurements taken for five values of the firing angle and six values of the voltage fundamental component. The results obtained using these algorithms show that the waveform measured by the analyzer is the closest to the waveform obtained considering only the first five odd harmonics computed by the genetic algorithm in [32]. The waveforms of the absorbed current by the rectifier, obtained using the *poly45* function or the proposed algorithm (described above) are similar.

The maximum relative error of the RMS values calculated for the current *I* with various algorithms used in this thesis is 1.5%, which shows that these results can be deemed similar in terms of electric installation operation.

In chapter 6, *Automatic reconfiguration of medium voltage power distribution networks in emergency mode*, a case study is presented for a looped medium voltage network with radial operation in which has been implemented an automatic reconfiguration system for the distribution network and a permanent short-circuit or a single-phase earth fault occurs. With these automations, a significant reduction in the amount of time needed to reconfigure the emergency networks is achieved, ranging from a few hours or even tens of hours under extreme weather conditions to approximately 20 seconds.

7.2 ORIGINAL CONTRIBUTIONS

The original contributions of this PhD thesis are related mainly to the frequency domain models of certain nonlinear devices in the power system. Starting from a paper published in 2017 [19], such models for a number of nonlinear loads have been built. The model elaboration method got continuously improved, starting from repeated simulations under various operating conditions [19], going on with measurements using a single-phase analyzer and then using a three-phase network analyzer. These models have been implemented in ADS software and have been used for analysis based on the harmonic balance method. Thus, we achieved a calculation time which is at least one order of magnitude shorter than when using usual models (described in the time domain) with the same ADS harmonic balance method.

The frequency domain models have been built for nonlinear loads, such as: compact fluorescent lamps, vacuum cleaners, microwave ovens and refrigerators, which all have in common non-controlled rectifiers powered from the power supply network. Considering that within a power network voltage may vary between 0.9 V_n and 1.1 V_n (V_n - the RMS nominal voltage value), we noticed that for this variation range of V_n these consumers have a linear dependency of the RMS values and phases of the current harmonics with respect to the RMS value and phase of the voltage fundamental component.

Moreover, frequency domain models for rectifiers with thyristors have been developed. In this case, the RMS values and phases of the current harmonics depend both on the RMS value of the voltage fundamental component and on the firing angle of thyristors. It has been found that, in some cases, these dependencies are nonlinear. The frequency domain models for these rectifiers are higher order polynomials in the RMS value V_1 of the voltage fundamental component at the rectifier's terminals and the value of the firing angle α. These polynomials' coefficients have been determined by two methods: using the *poly45* function in MATLAB and an original procedure similar to *poly45* based on a higher value count of V_1 and α. Due to the greater number of points on which the building of the two-variable polynomial representing the model relies on, this original procedure is more accurate than using *poly45*.

The efficiency of the analysis with harmonic balance in ADS using frequency domain models has also been investigate in a recently published paper [49], analyzing an unbalanced three-phase circuit with 150 capacitors, 150 diodes, 100 coils and 200 resistors through various methods. These results are shown in Table 7.1.

Table 7.1. **Efficiency of the analysis methods using TD and FD models [49]**

Analysis	**Duration**
HB ADS (FD models)	1.36s
HB ADS (TD models)	550.34s
Tran ADS (TD models)	10.76s
PSS HB Cadence (TD models)	215s
PSS tran Cadence (TD models)	5.39s
Tran Cadence (TD models)	6.88s

PSS-HB method from Cadence refers to a harmonic balance analysis method using time domain models, while PSS tran method from Cadence is the shooting method with Newton Raphson. It can be seen that the simulation time using this method is rather short, yet higher than the one required by HB method from ADS which uses the frequency domain models.

This example demonstrates the clear advantage of the models developed in this thesis.

If it is considered a low voltage network powered both from the national power system and from certain renewable power sources (photovoltaics and wind turbines) belonging to private entities that are mainly producing for their own consumption, the consumers in this network can be penalized in case of exceeding the harmonic pollution quotas presented in table 7.2. [51]

Table 7.2. **Compatibility thresholds for current harmonics (as % of the fundamental component) applicable to the consumer [51]**

Isc/Is	Harmonics degree (%)					Distortion factor (%)
	<11	11-16	17-22	23-34	≥35	
<20	4	2	1,5	0,6	0,3	5
20-50	7	3,5	2,5	1	0,5	8
50-100	10	4,5	4	1,5	0,7	12
100-1000	12	5,5	5	2	1	15
>1000	15	7	6	2,5	1,4	20

In this table Isc is the short-circuit current at the boundary between the consumer and the national power system (SEN); and Is is the rated current at the basic frequency, consistent with the connected load.

This kind of network can have various operation conditions, depending on: the occurrence of sufficient sun radiation that enables the photovoltaic sources to produce a certain minimal power, the occurrence of enough wind at speeds that enable the wind turbines to produce a certain minimal power, availability of private entities owning non-conventional power sources to activate these sources, the operating conditions of the consumers within this network. As the parameters in table 7.2 must be satisfied under any operating conditions, determination the optimal solution for compensating the current harmonics pollution [52] of the low voltage network must be done taking into account all these operating conditions. The final solution seems to be a set of active harmonic filters [52] to be placed so as to keep costs minimal and to guarantee they meet the requirements in table 7.2 under any network operating conditions.

7.3 FURTHER DEVELOPMENT PERSPECTIVES

If the models developed in this thesis are characterized by RMS values and phases of the current harmonics which depend on one (V_1) or two (V_1, α) parameters, there are certain applications in which RMS values and phases of the current harmonics may depend on three or more parameters. The third and the fourth parameters could be the load torque in a driving installation and the speed at which a motor revolves when actuated by the nonlinear consumer supplied by the power system.

The frequency domain models can be extended to medium and high voltage networks.

This type of models could also be used for simulating radiofrequency circuits using the harmonic balance method [17, 18].

PUBLISHED PAPERS

- Ștefănescu, V., Antohi, T., Poienar, M. - Automatic Reconfiguration of Medium Voltage Power Distribution Networks in Emergency Mode, International Conference and Exposition on Electrical and Power Engineering, 2018 – WOS: 000458752200107
- Gheorghe, A.G., Constantinescu, F., Marin, M.E., Ștefănescu, V., Vătășelu, G. - Frequency Domain Models for Nonlinear Home Appliance Devices, International Symposium on Fundamentals of Electrical Engineering, 2018 – WOS: 000480396400062
- Constantinescu, F., Gheorghe, A.G., Marin, M.E., Vătășelu, G., Ștefănescu, V., Bodescu, D. - New Models for Frequency Domain Simulation of Home Appliances Networks, International Symposium on Advanced Topics in Electrical Engineering, 2019 – WOS: 000475904500140
- Milici, M.R., Milici, L.D., Atănăsoae, P., Ștefănescu, V. - Studies on Energy Consumption Using Methods of Exponential Smoothing, International Symposium on Advanced Topics in Electrical Engineering, 2019 – WOS: 000475904500103
- Constantinescu, F., Rata, M., Enache, F.R., Vătășelu, G., Ștefănescu, V., Milici, D., Aramă, I. - Frequency Domain Models for Nonlinear Loads with Firing Angle Control Devices Part I Measured Data, International Conference on Engineering of Modern Electric Systems, 2019 – WOS: 000503434500061
- F. R. Enache, F. Constantinescu, M. Rață, G. Vătășelu, V. Ștefănescu, D. Milici, I. Aramă, Frequency Domain Models for Nonlinear Loads with Firing Angle control Devices Part II – Modeling, 2019 6th International Symposium on Electrical and Electronics Engineering (ISEEE), Galati, Romania, 18-20 October 2019 – WOS: 000614815800016
- Aramă, I., Găiceanu, M., Ștefănescu, V. - Management of the Electric Energy Distribution Network, International Conference on Engineering of Modern Electric Systems, 2019 – WOS: 000503434500062
- N. Badea, V. Ștefănescu, Evaluation of Harmonic Effects on the Power System Distribution, The Annals of „Dunarea de Jos" University of Galati, Fascicle III, 2020, Vol. 43, No. 1, ISSN 2344-4738, ISSN-L 1221-454X Electrotechnics, Electronics, Automatic Control, Informatics, Article DOI: https://doi.org/10.35219/eeaci.2020.1.02

REFERENCES

[1] J. Arrillaga, B. C. Smith, N. R.Watson, and A. R.Wood, *Power System Harmonic Analysis*. New York: Wiley, 1997.
[2] E. Acha and M. Madrigal, *Power System Harmonics: Computer Modelling and Analysis*. Hoboken, NJ: Wiley, 2001.
[3] IEEE Task Force on Harmonic Modeling and Simulation, "Modeling and simulation of the propagation of harmonics in electric power systems Part I: Concepts, models, and simulation techniques," *IEEE Trans. Power Del.*, vol. 11, no. 1, pp. 452–464, Jan. 1996.
[4] IEEE Task Force on Harmonic Modeling and Simulation, "Modeling and simulation of the propagation of harmonics in electric power systems Part II: Sample systems and examples," *IEEE Trans. Power Del.*, vol. 11, no. 1, pp. 466–474, Jan. 1996.
[5] A. Medina, "Harmonic simulation techniques (Methods & Algorithms)," presented at the IEEE Power Eng. Soc. Gen. Meeting, Denver, CO, USA, Jun. 6–10, 2004.
[6] IEEE Task Force on Harmonics Modeling and Simulation, ch. 5, "Harmonic analysis in frequency and time domains," IEEE PES 07TP184, 2007.
[7] IEEE Task Force on Interfacing Techniques for Simulation Tools, "Interfacing techniques for time-domain and frequency-domain simulation methods," *IEEE Trans. Power Del.*, vol. 25, no. 3, pp. 1796–1807, Jul. 2010.

[8] A. A. Mahmoud and R. D. Schultz, "Amethod for analyzing harmonic distribution in a.c. power systems," *IEEE Trans. Power App. Syst.*, vol. PAS-101, no. 6, pp. 1815–1824, Jun. 1982.
[9] T. J. Demsem, P. S. Bodger, and J. Arrillaga, "Three phase transmission system modelling for harmonic penetration studies," *IEEE Trans. Power App. Syst.*, vol. PAS-103, no. 2, pp. 310–317, Feb. 1984.
[10] Florin Constantinescu, Alexandru Gabriel Gheorghe, Miruna Nițescu, Viorel Constantin Marin, Anișoara Ionescu, „Simularea circuitelor (lucrări de laborator)", http://ferrari.lce.pub.ro/studenti. 2001-2020.
[11] F. Constantinescu, M. Nițescu, „Cursul de Electrotehnica, Partea I - Teoria Circuitelor Electrice", http://ferrari.lce.pub.ro/studenti, 2002-2020.
[12] V. R. Pandi, H. H. Zeineldin, W. Xiao, Determining Optimal Location and Size of Distributed Generation Resources Considering Harmonic and Protection Coordination Limits, IEEE Transactions on Power Systems, vol. 28, No. 2, May 2013, pp. 1245-1254.
[13] Task Force on Harmonics Modeling and Simulation, "Modeling and Simulation of the Propagation of Harmonics in Electric Power Networks, Part I: Concepts, Models, and Simulation Techniques", IEEE Transactions on Power Delivery, vol. 11, no. 1, January 1996.
[14] A. Medina, J. Segundo-Ramirez, P. Ribeiro, W. Xu, K. L. Lian, G. W. Chang, V. Dinavahi, and N. R. Watson, Harmonic Analysis in Frequency and Time Domain, IEEE Transactions on Power Delivery, vol. 28, no. 3, July 2013, pp. 1813-1821.
[15] P. Heikkila, M. Valtonen, T. Veijola, Harmonic balance of nonlinear circuits with multitone excitation, Proceedings of the European Conference on Circuit Theory and Design, 1991.
[16] K. L. Lian, P. W. Lehn, Harmonic Analysis of Single-Phase Full Bridge Rectifiers Based on Fast Time Domain Method, IEEE International Symposium on Industrial Electronics (ISIE 2006), July 9-12, 2006, Montreal, Quebec, Canada
[17] F. Constantinescu, A.-G. Gheorghe, M. Nitescu, Large signal analysis of RF circuits – an overview, Proceedings of ATEE (Advanced Topics in Electrical Engineering), Politehnica University, Bucharest, Romania, November 24-25, 2006.
[18] A. G. Gheorghe, F. Constantinescu, New Topics in Simulation and Modeling of RF Circuits, River Publishers, 2016.
[19] F. Constantinescu, A. G. Gheorghe, M. E. Marin, O. Taus, Harmonic balance analysis of home appliances power networks, 2017 14th International Conference on Engineering of Modern Electric Systems (EMES), June 1-2 2017, Oradea, Romania.
[20] A. Nassif, Modeling, Measurement and Mitigation of Power System Harmonics, PhD thesis in Electrical and Computer Engineering, University of Alberta, Edmonton, Canada, 2009.
[21] J. Yong,L. Chen, A. Nassif, W. Xu, A Frequency-Domain Harmonic Model for Compact Fluorescent Lamps, IEEE Transactions on Power Delivery, vol. 25, No. 2, April 2010, pp 1182-1189.
[22] A. G. Gheorghe, F. Constantinescu, M. E. Marin, V. Ștefănescu, G. Vătășelu, Frequency Domain Models for Nonlinear Home Appliance Devices, 2018 International Symposium on Fundamentals of Electrical Engineering (ISFEE), Bucharest, Romania, November 1-2, 2018.
[23]https://www.keysight.com/main/software.jspx?ckey=2212036&lc=eng&cc=RO&nid=-11143.0.00&id=2212036
[24] K. S. Kundert, A. Sangiovanni Vincentelli, "Simulation of Nonlinear Circuits in the Frequency Domain", IEEE Transactions on Computer-Aided Design, Vol. CAD-5, NO. 4, October 1986, pp. 521-535.
[25] R. Uhl, M. Mirz, T. Vandeplas, L. Barford, A. Monti, "Non-linear behavioral X-Parameters model of single-phase rectifier in the frequency domain", IECON 2016 - 42nd Annual Conference of the IEEE Industrial Electronics Society, pp. 6292 – 6297.
[26] M. Mirz, R. Uhl, T. Vandeplas, L. Barford, A. Monti, "Measurement-based parameter identification of non-linear polynomial frequency domain model of single-phase four diode bridge rectifier", Instrumentation and Measurement Technology Conference (I2MTC) 2017 IEEE International, pp. 1-6, 2017.
[27] S. A. Maas, Nonlinear microwave and RF circuits. Artech House, 2003.

[28] F. Constantinescu,. A G. Gheorghe, M. E. Marin, G. Vătășelu, V. Ștefănescu, D. Bodescu, New Models for Frequency Domain Simulation of Home Appliances Networks, 11th International Symposium on Advanced Topics in Electrical Engineering, March 28-30, 2019, Bucharest, Romania.
[29] F. Constantinescu, M. Nitescu, C. V. Marin, A Glimpse into some Aspects of Nonlinear Circuit Analysis, The National Symposium of Theoretical Electrical Engineering (SNET), May 12-14 , 2005.
[30] A. Semlyen, J. Arrillaga, "Newton-type algorithms for the harmonic phasor analysis of non-linear power circuits in periodical steady state with special reference to magnetic non-linearities," IEEE Trans. Power Delivery, vo. 3, No. 3 (July 1988), pp. 1090-1098.
[31] http://www.euedia.tuiasi.ro/lab_ep/ep_files, Technical University "Gheorghe Asachi", Iaşi, Romania, Faculty of Electrical Engineering and Power Engineering, Power Electronics Laboratory (in Romanian).
[32] A. Enache, T. Petrescu, F.R. Enache, F.G. Popescu, Spectrum Computation for Periodic Analog Signals Using Genetic Algorithms, ICATE 2014 - International Conference on Applied and Theoretical Electricity, Craiova, Romania, 23-25 October, 2014.
[33] F. Constantinescu, M. Rață, F. R. Enache, G. Vătășelu, V. Ștefănescu, D. Milici, I. Aramă, Frequency Domain Models for Nonlinear Loads with Firing Angle control Devices Part I – Measurements, 2019 15th International Conference on Engineering of Modern Electric Systems (ICEMES), Oradea, Romania, 13-14 June 2019.
[34] F. R. Enache, F. Constantinescu, M. Rață, G. Vătășelu, V. Ștefănescu, D. Milici, I. Aramă, Frequency Domain Models for Nonlinear Loads with Firing Angle control Devices Part II – Modeling, 2019 6th International Symposium on Electrical and Electronics Engineering (ISEEE), Galati, Romania, 18-20 October 2019.
[35] E. Stedin, Voorkom afsluiting van elektriciteit en/of gas, at https://www.stedin.net/aansluiting/energie-behouden/,
[36] ***, China Electric Power Wquipment and Technology Co. Ltd., at http://www.cet.sgcc.com.cn/html/zdzb/col1310000067/.
[37] G. Cartina, G. Grigoras, and E.C. Bobric– "Clustering techniques for energy losses evaluation in distribution networks", Published in: 2009 IEEE PowerTech, 2009, p. 1-5.
[38] P. Atanasoae and R. Pentiuc "Indices for the power quality monitoring in the Romanian Power Transmission System". Published in: 16th International Conference on Harmonics and Quality of Power (ICHQP) 2014, p. 68-71.
[39] M. Cenușă, M. Poienar and D. L. Milici. Study of a system for reducing electricity losses. In: International Conference on Development and Application Systems 14th Edition, May 24-26, 2018, Suceava, Romania.
[40] R. Berthier, W.H. Sanders and H. Khurana, Intrusion Detection for Advanced Metering Infrastructures, in First IEEE International Conference on Smart Grid Communications, 2010.
[41] D. Calitoiu, L. D. Milici, Modeling with Non-cooperative Agents: Destructive and Non-Destructive Search Algorithms for Randomly Located Objects, in Search Algorithms and Applications, edited by Nashat Mansour, INTECH, 2011.
[42] L. D. Milici, M. R. Milici, „Sisteme de monitorizare şi transmisii de date – structuri şi principii de funcţionare", Editura Didactică şi Pedagogică, Bucureşti, 2014.
[43] L. D. Milici, M. R. Milici, W. Flore, To use a microcontroller in a small energy powerplant management, International Conference and Exposition on Electrical and Power Engineering - EPE 2014, vol: IEEE: CFP1447S-USB, pag: 1141-1147
[44] European Comission – Vision and Strategy for Europe's Electricity Networks of the Future, Platforma Tehnologică Europeană SmartGrids, 2006.
[45] European Comission – Strategic Deployment Document for Europe's Electricity Networks of the Future, Platforma Tehnologică Europeană SmartGrids, 2008.
[46] EPRI – The Integrated Energy and Communication Systems Architecture, Vol. IV, Technical Analysis, Electric Power Research Institute, 2004.
[47] M. Sănduleac, A. Pop and R. Strutu, „Contoare inteligente şi Reţele Energetice Inteligente", Conferinţa Reţele Energetice Inteligente, Sibiu · 21 - 23 Septembrie 2010.

[48] V. Ştefãnescu, T. Antohi and M. Poienar, Automatic Reconfiguration of Medium Voltage Power Distribution Networks in Emergency Mode, 2018 10th International Conference on Electrical and Power Engineering (EPE), October 18-19 2018, Iași, Romania.
[49] Alexandru Gabriel Gheorghe, Florin Constantinescu, Mihai Eugen Marin, Time Domain and Frequency Domain Models for Analysis of Nonlinear Power Networks of Home Appliances, International Symposium on Signals, Circuits and Systems, July 15-16 2021, Iasi, Romania.
[50] O. S. Taus - Modelarea și analiza în domeniul frecvenței a unor circuite cu componente pasive neliniare, Teză de doctorat, Universitatea POLITEHNICĂ București, 2020.
[51] PE 143/94 - Normativ privind limitarea regimului nesimetric și deformant în rețelele electrice, Regia Autonomă de Electricitate RENEL, București, 1994.
[52] Nicolae Badea, Alexandra Dusa și Nicu Roman, Power Quality Comparative Analysis between UPF and SAPF, Journal of Energy and Power Engineering, Volume 15, Number 4, April 2021 (Serial Number 157).